

# Correlation of ZnO Surface Morphology and Sensing Performance of EGFET Nitrate Sensor

A. B. Rosli, S. B. Hashim, R. A. Rahman, S. H. Herman, W. F. H. Abdullah\*  
Integrated Sensors Research Lab, School of Electrical Engineering,  
Universiti Teknologi MARA, 40450 Shah Alam, Selangor, Malaysia  
\*wanfaz@uitm.edu.my

Z. Zulkifli  
NANO-ElecTronic Centre, School of Electrical Engineering,  
Universiti Teknologi MARA, 40450, Shah Alam, Selangor, Malaysia.

S. H. Herman  
Microwave Research Institute, Universiti Teknologi MARA, 40450,  
Shah Alam, Selangor, Malaysia

## ABSTRACT

*Zinc oxide (ZnO) sensing electrode (SE) for extended gate field-effect transistor (EGFET) nitrate sensor was deposited on top of indium tin oxide (ITO) substrate using two different methods which were spin coating and chemical bath deposition (CBD) methods. To investigate the correlation between physical properties and sensing performance based on different growth methods, the deposited samples were characterized on its surface morphology using field emission scanning electron microscopy (FESEM). The ZnO sample deposited using spin coating showed an agglomerated structure while ZnO nanorods (ZnR) were observed on the ITO sample using the CBD method. Before the nitrate sensing measurement, the polyvinylpyrrolidone (PVP) polymer was deposited on top of ZnO samples for both methods at different concentrations of 2, 4 and 6 wt%. Both samples showed the ability as a SE for the EGFET nitrate sensor with 4 wt% PVP showed the optimum sensing behaviour. Based on the results obtained, the sensitivity of the ZnO SE using spin coating and ZnR by CBD method were 3.9 and 59.8 mV/dec, respectively, with the linearity 0.92919 and 0.98414, respectively. It was evident that nitrate sensing performance depended on the SE's growth*

*morphology. The high sensitivity of ZnR SE was related to nanorods structure that provides a high surface area and facilitates more contact between SE and nitrate solution for ion adsorptions. As a comparison, a sample without ZnO material with 4 wt% of PVP concentration was deposited and tested for nitrate sensing performance. The sensitivity and linearity of PVP sample were 20.60 mV/dec and 0.76601. It was proven that the ZnO material plays important role in increasing the nitrate sensing performance.*

**Keywords:** ZnO; Thin Film; Nanorods; EGFET; Nitrate Sensor

## Introduction

Nitrate is one of the crucial elements that play an important role in living things' physiological and biochemical functions. This nitrate is required by plants for healthy growth and development. Meanwhile, for humans, dietary nitrates, which are mostly found in green leafy vegetables, water and fruits are turned into nitric oxide have beneficial effects such as lowering blood pressure, preventing cardiovascular diseases and boosting blood flow. However, anthropogenic activities based on nitrate in wide fields especially agriculture, food processing and industries lead to an excess amount of nitrate in ecosystems that are harming the environment and human health [1]. Therefore, monitoring concentration levels in the environment are becoming particularly crucial.

Various analytical procedures for nitrate detection have been developed and reported such as colorimetric, spectrometric and ion chromatography [2]-[4]. However, the existing methods require complex instruments, a vast workspace, and professional hands to operate [5]-[7]. These drawbacks caused the existing methods expensive and time-consuming. Hence, electrochemical techniques are appealing options in replacement to the existing techniques. This technique is particularly interesting because they enable the construction of integrated chemical/electrochemical sensors using ion-sensitive electrodes (ISE). As a result, potentiometric, amperometric, and impedimetric detection methods for nitrogen-based ions have been thoroughly developed [8]. The potentiometric method based on extended-gate field-effect transistor (EGFET) has gained considerable attention since this technique offers lots of advantages such as simple and flexible connection, insensitive to light and temperature, and low cost [9]-[11]. This EGFET is made up of an ion-sensitive electrode which is also known as a sensing electrode (SE) and a metal-oxide-semiconductor field-effect transistor (MOSFET) device. Only SE is directly immersed in measurement solutions while MOSFET is isolated. Based on previous research on EGFET, most researchers are focusing on SE since this part is believed to improve sensing performance [12]-[14]. Metal oxide material has received significant attention as SE due to its excellent properties

in terms of electrical and chemical [15]-[17]. Among these metal oxides, ZnO is one of the best candidates due to its nanostructures facilitating a high surface-to-volume ratio and fast electron communication for excellent sensing performance [18]. This variety of ZnO nanostructures can be synthesized using a wide range of methods such as physical vapour deposition (PVD), hydrothermal, sol-gel and chemical bath deposition (CBD). Spin coating and CBD methods are well-known methods to synthesize ZnO nanoparticles and nanostructures, respectively. The sol-gel spin coating technique is a simple deposition method with a higher throughput that does not necessitate the use of time-consuming vapour phase deposition equipment [19]. Meanwhile CBD method has several advantages compared to other nanomaterial synthesis methods such as simplicity, reliability and versatility for large-scale production and can be synthesized at low temperatures [20]-[21]. Besides that, this CBD method also exhibits high purity and controlled growth of ZnO nanostructure's size and morphologies.

Nowadays, the combination of metal oxide with polymeric material as SE has become a popular option for in-situ ionic sensors due to its tunable properties and robustness. This polymer is used to modify the SE in terms of electrical, mechanical, structural and surface morphology properties [1]. The major disadvantages associated with metal oxide sensors are their poor selectivity, therefore, the cooperation of polymer into the metal oxide sensing layer improves the selectivity of target ion [22]-[23]. Polyvinyl pyrrolidone (PVP) has several advantages in terms of flexibility, environmental stability, non-toxic and biodegradable. Tang et al. [24] have reported their work on nitrate detection using PVP based on a fluorescent sensor. From their research, it shows that the PVP polymer can detect nitrate ions.

In this work, the ZnO SE based on the EGFET sensor has been synthesized using two different methods namely spin coating and CBD method with varied PVP concentrations at 2, 4 and 6 wt%. The correlation of ZnO growth morphology with nitrate sensing performance at optimum PVP concentration has been observed.

## **Experimental**

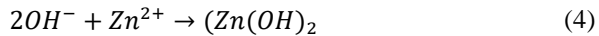
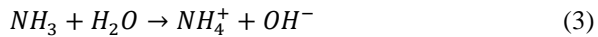
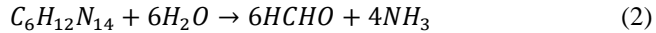
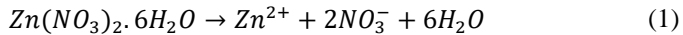
In this research 1 x 2 cm<sup>2</sup> ITO substrate was used to deposit ZnO SE. However, only 1 x 1 cm<sup>2</sup> of ITO substrate was used to deposit ZnO SE using 2 different methods which are the spin coating technique and CBD method respectively. The rest of the 1 x 1 cm<sup>2</sup> ITO substrate was insulated during the deposition process for EGFET wire connection during sensor measurement. The ZnO deposited by the spin coating technique was used as a seed layer for ZnO nanostructures growth using the CBD method. The fabrication of ZnO SE is thoroughly explained in detail below.

### Deposition process of ZnO seed layer

Zinc acetate dihydrate ( $ZnAc_2$ ), 2-methoxyetanol ( $C_3H_5OH$ ) and monoethanolamine (MEA) were used as precursor, solvent and stabilizer respectively. All the materials were mixed to form 0.4 M of ZnO solutions. Then, the mixture solution has undergone an aging process on a hot plate at 80 °C for 3 hours. The heat was then turned off and the mixture solution was continued to be stirred for another 24 hours to form a homogenous and clear ZnO solution. The ZnO solution was deposited on a 1 x 1 cm<sup>2</sup> ITO substrate using a spin coater at 3000 rpm. Finally, the deposited samples were dried for 10 minutes at 150 °C before being annealed for 1 hour at 500 °C.

### Deposition process of ZnO nanostructures

A two-step method was used to deposit ZnO nanostructures. First, the ZnO seed layer was deposited using the spin coating technique as explained above and followed by the growth of the ZnO nanostructures by CBD method. In this process, the zinc nitrate hexahydrate ( $Zn(NO_3)_2 \cdot 6H_2O$ ) was used as a precursor while hexamethylenetetramine (HMT, ( $C_6H_{12}N_4$ )) was used as a stabilizer. Before the deposition process,  $Zn(NO_3)_2 \cdot 6H_2O$  and  $C_6H_{12}N_4$  were dissolved in 500 ml deionized (DI) water to form 0.1 M of ZnO solution. Then, the mixture solution was sonicated for 30 min at 50 °C in an ultrasonic bath. After the sonicated process, the solution underwent a stirring process at 300 rpm for 3 hours. The stirred temperature was set at room temperature. After that, the ITO substrate containing the ZnO layer which was deposited before using spin coating was used as a seed layer and immersed in prepared solutions. All the prepared solutions were placed in the water bath for 1 hour at 95 °C. After the deposition process, the deposited ZnO nanostructures samples were dried for 10 min at 50 °C followed by an annealing process at 500 °C for 1 hour. The chemical reaction involved in Zn production is explained in Equations (1) to (5) below [25]:



The dissolution of  $Zn(NO_3)_2 \cdot 6H_2O$  in DI water produced  $Zn^{2+}$  for the formation of ZnO nanorods as shown in Equation (1) while the dissolution of  $C_6H_{12}N_4$  in DI water yielding formaldehyde (HCHO) and ammonia ( $NH_3$ ) as shown in Equation (2). Based on Equation (3), ammonium ( $NH_4^+$ ) and

hydroxyl (OH) ions were formed when  $\text{NH}_3$  dissolves in water ( $\text{H}_2\text{O}$ ). The produced  $\text{OH}^-$  was reacted with the  $\text{Zn}^{2+}$  and formed the zinc hydroxide ( $(\text{Zn}(\text{OH})_2)$ ) that finally decomposed into ZnR and  $\text{H}_2\text{O}$  as described in Equation (4) and Equation (5), respectively.

### **Deposition process of polyvinylpyrrolidone (PVP) polymer**

In this work, polyvinylpyrrolidone (PVP) was deposited on top of the ZnO layer deposited using both methods by spin coating technique. PVP was prepared by mixing the PVP powder with 20 ml of solvent. The absolute ethanol and DI water were used as solvents with a ratio of 8:2 respectively. Then, the prepared PVP solution was stirred for an hour at 350 rpm. After the stirring process, the prepared PVP solution was dropped on the ZnO layer and ZnO nanostructures using spin coating. The spin coating was set for 2 cycles at 500 rpm for 10 sec and 3000 rpm for 30 sec respectively. At the end of the process, the prepared samples were dried on a hot plate at 100 °C for 10 min. As-deposited sample without ZnO material was prepared for comparison.

### **Samples characterization**

The surface morphology of deposited samples was observed using Field-Emission Scanning Electron Microscope (FESEM) in order to study the relationship of growth morphology with sensing performance. For nitrate sensing performance measurement, the deposited samples were connected to a copper wire and insulated using epoxy to prevent the solution from leaking during the measurement process. The gate of a commercialized n-type FET was connected to the end of the copper wire. The deposited sample and commercialized silver/silver chloride (Ag/AgCl) reference electrode (RE) were immersed together into the different concentrations of nitrate solution varied from 0 to 100 ppm. The nitrate measurement setup was shown in Figure 1. The current-voltage ( $I_d$ - $V_{\text{ref}}$ ) properties of the deposited samples were measured using a Keysight B1500A Semiconductor Device Analyzer. The gate voltage versus nitrate concentration graph was plotted based on transfer curve measurement at 100  $\mu\text{A}$  drain current for each nitrate concentration. The sensor sensitivity was calculated using the slope of the  $V_{\text{ref}}$  -nitrate concentration graph, and the linearity was determined using linear regression ( $R^2$ ).

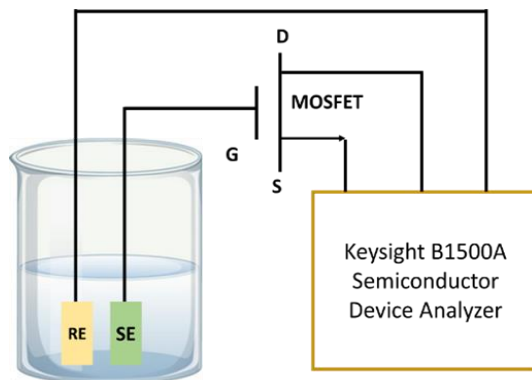


Figure 1: EGFET setup for nitrate sensing measurement

## Result and Discussions

### Surface morphology of deposited ZnO SE

Figure 2 shows the surface morphology of the ZnO layer using (a) spin coating and (b) CBD methods respectively. The inset of Figure 2b shows the cross-section layer of the ZnO sample deposited using the CBD method. From Figure 2a, the ZnO agglomerated roughly on ITO substrate and formed the granular structure of ZnO particles while Figure 2b shows that the ZnO grown uniformly and formed ZnO nanorods (ZnR). This ZnR was observed on a cross-section image as shown in the inset of Figure 2b.

The formation of the granular structure of ZnO particles using spin coating is due to a continuous coarsening process that occurs at the dried and final annealing process of the samples. The agglomeration of small grains under the influence of thermal energy results in the formation of large grains [26]. The ZnO deposited by spin-coated was used as a seed layer template for CBD deposition acts as nucleation site for the growth of ZnR by reducing the inherent lattice mismatch [27]. This ZnR mechanism can be explained by Ostwald ripening process<sup>3</sup>. According to Ostwald' ripening process [28], the molecules on the surface of a small particle tend to detach and diffuse into the solution, increasing the concentration of free molecules in solution. At the supersaturated point, these molecules tend to condense on the surfaces of larger particles. As a result, all smaller particles diminish while larger particles develop. ZnR will then "push on" from both the prepared sites and the aggregated ones. Since larger particles are more energetically stable than smaller ones, this process is also thermodynamically spontaneous [28].

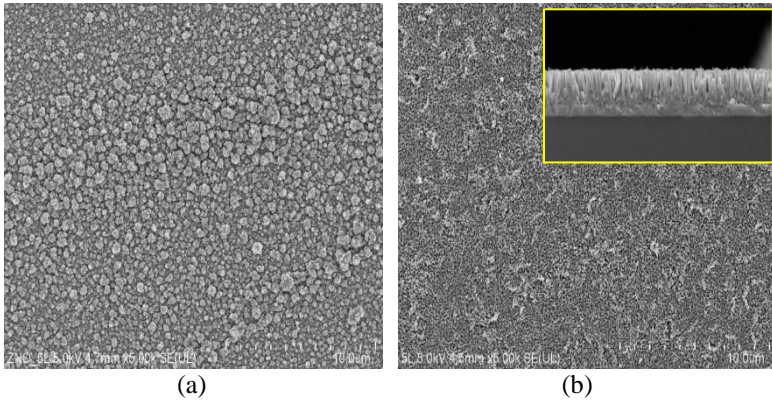


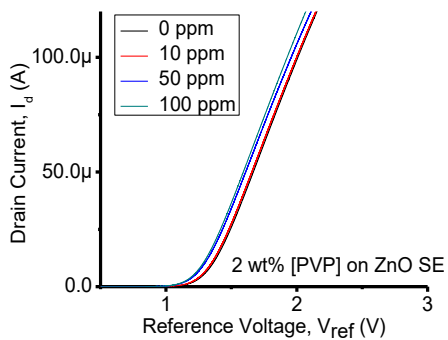
Figure 2: Surface morphology for; (a) ZnO seed layer and, (b) ZnR inset with the cross-section for ZnR

### ZnO SE EGFET sensor characterizations

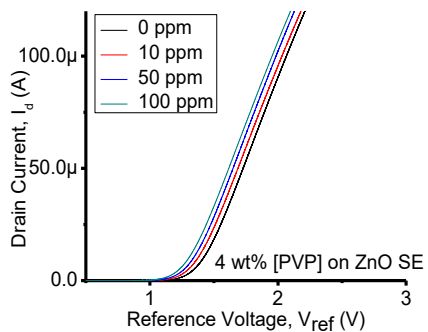
The deposited samples were characterized on EGFET nitrate sensor characteristics in terms of the transfer characteristic, sensitivity, and linearity respectively. A detailed explanation of each characterization is discussed below.

#### Transfer characteristic

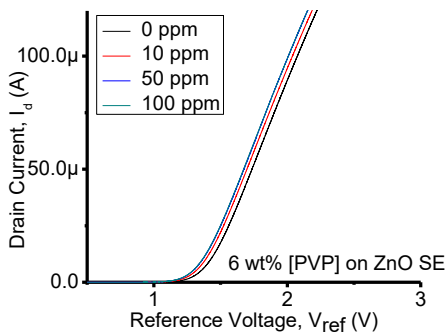
The transfer characteristic of drain current versus voltage reference,  $V_{ref}$  for ZnO and ZnR was examined using a Keysight B1500A Semiconductor Device Analyzer. In this measurement, the  $V_{ref}$  was swept from 0 to 3 V. Figure 3 and Figure 4 show the transfer curve characteristic for ZnO and ZnR SE at a) 2, b) 4 and c) 6 wt% of PVP concentration, respectively. From both Figure 3 and Figure 4, it can be seen obviously only samples 4 wt% have a normal voltage shifted from right to the left. At 4 wt% PVP concentration, the shifted gap difference of sample ZnO SE is equally for each nitrate concentration. However, for ZnR sample at 4 wt% PVP concentration, it can be seen in Figure 4b the gap between  $V_{ref}$  at 50 ppm and 100 ppm quite large compared to ZnO SE (Figure 3b). While for 2 and 4 wt% samples, both ZnO and ZnR SE shows the overlapping transfer curve between 0 and 10 ppm and also 50 and 100 ppm respectively. This overlapping curve indicating that sample at 2 and 4 wt% of PVP concentration is not suitable as a sensor device. Based on this result, the  $V_{ref}$  for each concentration was observed and plotted versus nitrate concentration in  $\log_{10}$  as shown in Figure 5 and Figure 6, respectively, then the nitrate sensitivity of the samples was calculated from the slope of  $V_{ref}$ - $\log_{10}$  NO<sub>3</sub><sup>-</sup> plot.



(a)



(b)



(c)

Figure 3: ZnO seed layer transfer characteristics ( $I_d$ - $V_{ref}$ ) of ZnO SE at a) 2 wt%, b) 4 wt% and c) 6 wt% of PVP concentration

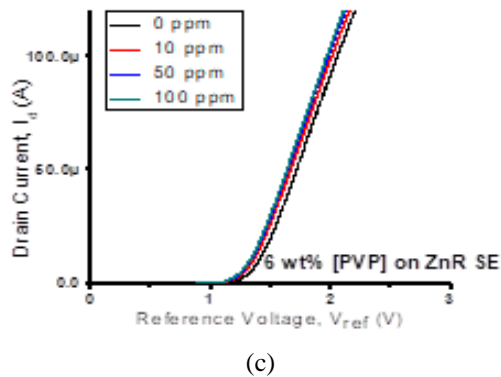
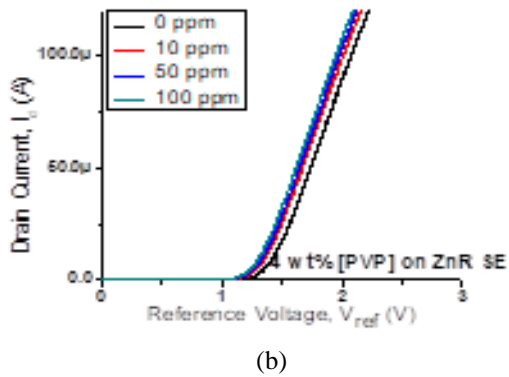
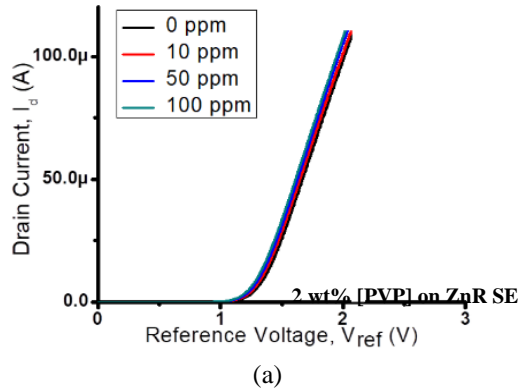


Figure 4: ZnR transfer characteristics ( $I_d$ - $V_{ref}$ ) of ZnO SE at a) 2 wt%, b) 4 wt% and c) 6 wt% of PVP concentration

### Sensitivity and linearity

Figures 5a, 5b and 5c show the  $V_{ref} \cdot \log [NO_3^-]$  graph plotted for ZnO SE deposited using spin coating technique at 2, 4, and 6 wt% PVP concentration, respectively. The obtained sensitivity and linearity values from these results were tabulated in Table 1.

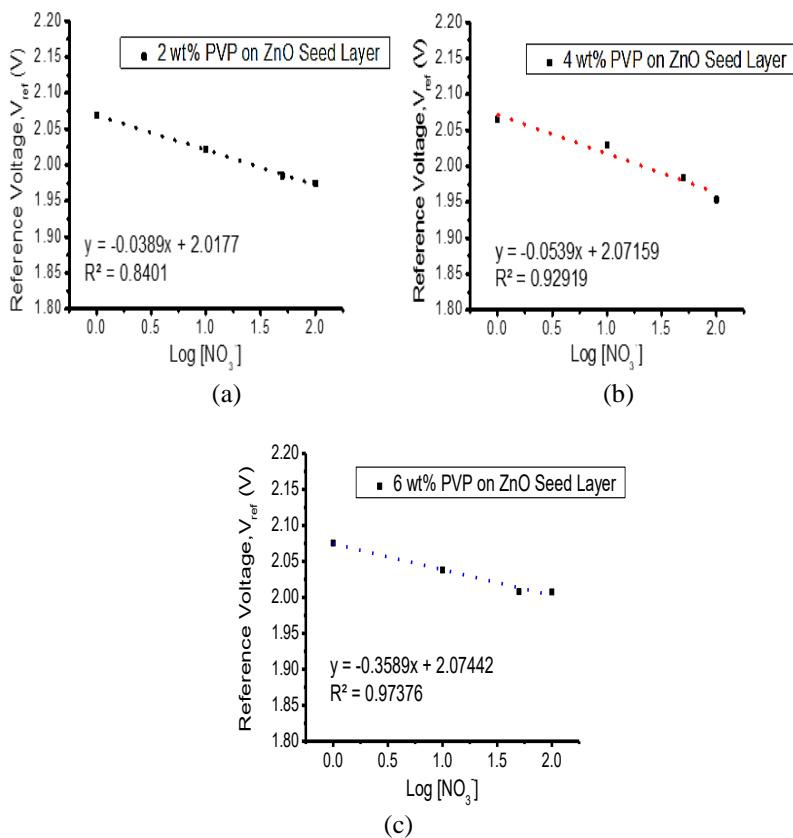


Figure 5:  $V_{ref}$ - $\log [NO_3^-]$  graph of ZnO sensing electrode deposited using spin coater technique at (a) 2, b) 4 and c) 6 wt% of PVP concentration

From Table 1, the sensitivity of ZnO SE deposited using spin coating at 2, 4 and 6 wt% PVP concentrations are 38.9, 53.9, and 35.89 mV/dec while its linearity is 0.84010, 0.92919, and 0.97376, respectively. These results show that 4 wt% PVP concentration gives the optimum sensitivity value for nitrate sensing performance.

Table 1: The sensitivity and linearity values of ZnO sensing electrode deposited using spin coating technique at different PVP concentrations

PVP Concentration (w%)	Sensitivity (mv/Dec)	Linearity
2	38.90	0.84010
4	53.90	0.92919
6	35.89	0.97376

The same process has been done for ZnR SE at different PVP wt% concentrations, as shown in Figure 6. The obtained results for ZnR SE nitrate detection are tabulated in Table 2. From this table, it can be seen that the optimum sensing performance for ZnR also is obtained at 4 wt% with sensitivity and linearity of 59.8 mV/dec and 0.98413 respectively. This result proved that the sensing performance of deposited ZnO is dependent on the surface structure. The ZnR structure improves the sensitivity and linearity value of the nitrate sensor compared to ZnO agglomeration particles. This is due to ZnR having a high surface-to-area ratio that provided a high surface area for ion reaction. Both samples ZnO and ZnR SE shows the decrement of sensitivity values when the PVP concentration wt% was increased to 6 wt%. This may be due to an increase of SE thickness and resistivity [29] which results in a decrease of the potential voltage produced.

To confirm that high sensitivity comes from ZnO material, a sample without ZnO was deposited using the 4 wt% of PVP concentration. Summarized data on sensitivity and linearity for PVP, ZnO and ZnR SE are tabulated in Table 3, for comparison. From the results obtained the sensitivity and linearity of the PVP sample is 20.60 mV/dec and 0.76601. The sensitivity and linearity values of the PVP sample are the lowest compared to the ZnO and ZnR SE. This result proved that the high sensitivity of nitrate sensing comes from the ZnO material itself.

Comparing the sensitivity and linearity of ZnO and ZnR SE, it can be seen that both samples work very well as nitrate sensing electrodes. The value of sensitivity was improved from 53.90 to 59.8 mV/dec for ZnR SE compared to ZnO SE. While for linearity, the value was improved from 0.92919 to 0.98413. This improvement in nitrate sensing performance was attributed to a different kind of surface morphology even though the same material is used. The deposited ZnR SE exhibits a high surface area to volume ratio that facilitates more surface possibilities for the nitrate ions binding, resulting in high sensitivity of nitrate detection. Meanwhile, the flat surface of ZnO SE caused a less exposed surface for nitrate ions reaction. Furthermore, the existence of thousands of nanorod structures on the ZnO seed layer surface acting as an independent electrode for the sensing reaction may contribute to a highly sensitive response compared to ZnO SE [30].

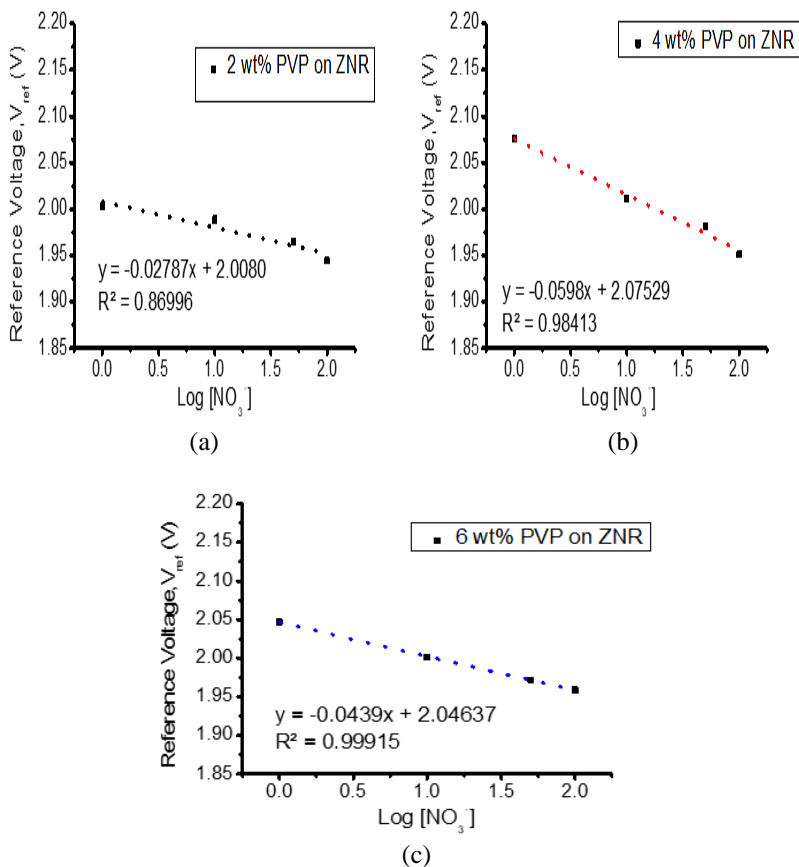


Figure 6:  $V_{ref}$ - $\text{Log}[\text{NO}_3^-]$  graph of ZnR sensing electrode deposited using spin coater technique at (a) 2, b) 4 and c) 6 wt% of PVP concentration

Table 2: The sensitivity and linearity values of ZnR sensing electrode deposited using spin coating technique at different PVP concentrations

PVP Concentration (w%)	Sensitivity (mv/Dec)	Linearity
2	27.87	0.86996
4	59.8	0.98413
6	43.90	0.99915

Table 3: Comparison on sensitivity and linearity values of the EGFET sensing electrode at 4 % PVP concentration

Type of SE	Sensitivity (mv/Dec)	Linearity
PVP Sample	20.60	0.76601
ZnO Seed Layer	53.90	0.92919
ZnR	59.80	0.98413

## Conclusion

ZnO layer and ZnR were successfully deposited on ITO substrate as EGFET nitrate sensor SE using spin coater and CBD methods. The surface morphology of ZnO SE was dependent on the deposition method. Agglomerate particles of ZnO were obtained using the spin coating technique, while for the samples deposited using the CBD method, the ZnR was observed. The PVP concentration effect at 2, 4 and 6 wt% on nitrate sensing performance were investigated for both deposited ZnO SE using an EGFET setup. Both samples showed the optimum nitrate sensitivity values at 4 wt% of PVP concentration. The performance of ZnO SE as a nitrate sensor shows a correlation with the growth morphology. The sensitivity of ZnO SE using the spin coating technique was 53.9 mV/dec while ZnR SE obtained from the CBD technique was 59.8 mV/Dec. Nanorod structure enhanced the sensor performance by facilitating more reaction sites due to the high surface-to-volume ratio. The sensitivity of the sample without ZnO (PVP sample) was 20.6 mV/Dec. These results proved that the ZnO material has a significant effect on nitrate sensing behavior.

## Acknowledgment

This research was funded partially by the Ministry of Science, Technology and Innovation (MOSTI) under International Collaboration Fund (ICF) grant (100-TNCPI/GOV 16/6/2 (008/2020)).

## References

- [1] R. K. A. Amali, H. N. Lim, I. Ibrahim, N. M. Huang, Z. Zainal, and S. A. A. Ahmad, "Significance of nanomaterials in electrochemical sensors for nitrate detection: A review," *Trends in Environmental Analytical Chemistry*, vol. 31, pp. e00135, 2021. <https://doi.org/10.1016/j.teac.2021.e00135>.

- [2] M. Sepahvand, F. Ghasemi, and H. M. Seyed Hosseini, "Plasmonic nanoparticles for colorimetric detection of nitrite and nitrate," *Food and Chemical Toxicology*, vol. 149, pp. 112025, 2021. <https://doi.org/10.1016/j.fct.2021.112025>.
- [3] A. Drolc and J. Vrtovšek, "Nitrate and nitrite nitrogen determination in waste water using on-line UV spectrometric method," *Bioresource Technology*, vol. 101, no. 11, pp. 4228-4233, 2010. <https://doi.org/10.1016/j.biortech.2010.01.015>.
- [4] M.-Y. Kim et al., "Highly stable potentiometric sensor with reduced graphene oxide aerogel as a solid contact for detection of nitrate and calcium ions," *Journal of Electroanalytical Chemistry*, vol. 897, p. 115553, 2021. <https://doi.org/10.1016/j.jelechem.2021.115553>
- [5] G. Li et al., "Electrochemical detection of nitrate with carbon nanofibers and copper co-modified carbon fiber electrodes," *Composites Communications*, vol. 29, pp. 101043, 2022. <https://doi.org/10.1016/j.coco.2021.101043>.
- [6] N. Nontawong et al., "Smart sensor for assessment of oxidative/nitrative stress biomarkers using a dual-imprinted electrochemical paper-based analytical device," *Analytica Chimica Acta*, vol. 1191, pp. 339363, 2022. <https://doi.org/10.1016/j.aca.2021.339363>
- [7] J. F. Tan, A. Anastasi, and S. Chandra, "Electrochemical detection of nitrate, nitrite and ammonium for on-site water quality monitoring," *Current Opinion in Electrochemistry*, vol. 32, pp. 100926, 2022/04/01/2022. <https://doi.org/10.1016/j.coelec.2021.100926>
- [8] M. Joly, M. Marlet, C. Durieu, C. Bene, J. Launay, and P. Temple-Boyer, "Study of chemical field effect transistors for the detection of ammonium and nitrate ions in liquid and soil phases," *Sensors and Actuators B: Chemical*, vol. 351, pp. 130949, 2022. <https://doi.org/10.1016/j.snb.2021.130949>
- [9] C.-W. Wang and T.-M. Pan, "Structural properties and sensing performances of CoNxOy ceramic films for EGFET pH sensors," *Ceramics International*, vol. 47, no. 18, pp. 25440-25448, 2021. <https://doi.org/10.1016/j.ceramint.2021.05.266>
- [10] P. Sharma et al., "Hydrogen ion sensing characteristics of Na3BiO4–Bi2O3 mixed oxide nanostructures based EGFET pH sensor," *International Journal of Hydrogen Energy*, vol. 45, no. 37, pp. 18743-18751, 2020. <https://doi.org/10.1016/j.ijhydene.2019.07.252>.
- [11] L. H. Slewa, T. A. Abbas, and N. M. Ahmed, "Synthesis of quantum dot porous silicon as extended gate field effect transistor (EGFET) for a pH sensor application," *Materials Science in Semiconductor Processing*, vol. 100, pp. 167-174, 2019. <https://doi.org/10.1016/j.mssp.2019.04.045>
- [12] M. Das, T. Chakraborty, C. Y. Lin, R.-M. Lin, and C. H. Kao, "Screen-printed Ga2O3 thin film derived from liquid metal employed in highly sensitive pH and non-enzymatic glucose recognition," *Materials*

- Chemistry and Physics*, vol. 278, pp. 125652, 2022. <https://doi.org/10.1016/j.matchemphys.2021.125652>
- [13] T. M. Pan, C. H. Lin, and S. T. Pang, "Structural properties and sensing performance of TaOx/Ta stacked sensing films for extended-gate field-effect transistor pH sensors," *Journal of Alloys and Compounds*, vol. 903, p. 163955, 2022. <https://doi.org/10.1016/j.jallcom.2022.163955>
- [14] T.-M. Pan, Y.-S. Huang, and J.-L. Her, "Super-Nernstian pH sensitivity of TbTaO4 sensing film for a solid-state pH sensor," *Materials Chemistry and Physics*, vol. 275, pp. 125284, 2022. <https://doi.org/10.1016/j.matchemphys.2021.125284>
- [15] L. H. Slewa, T. A. Abbas, and N. M. Ahmed, "Effect of Sn doping and annealing on the morphology, structural, optical, and electrical properties of 3D (micro/nano) V2O5 sphere for high sensitivity pH-EGFET sensor," *Sensors and Actuators B: Chemical*, vol. 305, pp. 127515, 2020. <https://doi.org/10.1016/j.snb.2019.127515>
- [16] H. A. Khizir and T. A.-H. Abbas, "Hydrothermal synthesis of TiO2 nanorods as sensing membrane for extended-gate field-effect transistor (EGFET) pH sensing applications," *Sensors and Actuators A: Physical*, pp. 113231, 2021. <https://doi.org/10.1016/j.sna.2021.113231>
- [17] Q. Lu *et al.*, "Mixed potential type NH3 sensor based on YSZ solid electrolyte and metal oxides (NiO, SnO2, WO3) modified FeVO4 sensing electrodes," *Sensors and Actuators B: Chemical*, vol. 343, pp. 130043, 2021. <https://doi.org/10.1016/j.snb.2021.130043>
- [18] F. Zhou *et al.*, "A novel flexible non-enzymatic electrochemical glucose sensor of excellent performance with ZnO nanorods modified on stainless steel wire sieve and stimulated via UV irradiation," *Ceramics International*, vol. 46, no. 10, 2022. <https://doi.org/10.1016/j.ceramint.2022.01.332>
- [19] U. Chaitra, D. Kekuda, and K. Mohan Rao, "Effect of annealing temperature on the evolution of structural, microstructural, and optical properties of spin coated ZnO thin films," *Ceramics International*, vol. 43, no. 9, pp. 7115-7122, 2017. <https://doi.org/10.1016/j.ceramint.2017.02.144>
- [20] Z. Zheng, J. Lin, X. Song, and Z. Lin, "Optical properties of ZnO nanorod films prepared by CBD method," *Chemical Physics Letters*, vol. 712, pp. 155-159, 2018. <https://doi.org/10.1016/j.cplett.2018.09.006>
- [21] M. Kardeş, H. Yılmaz, and K. Öztürk, "Pure and cerium-doped ZnO nanorods grown on reticulated Al2O3 substrate for photocatalytic degradation of Acid Red 88 azo dye," *Ceramics International*, vol. 48, no. 5, pp. 7093-7105, 2022. <https://doi.org/10.1016/j.ceramint.2021.11.269>
- [22] J. Kim, Q. Liu, and T. Cui, "Solution-gated nitrate sensitive field effect transistor with hybrid film: CVD graphene/polymer selective membrane," *Organic Electronics*, vol. 78, pp. 105551, 2020. <https://doi.org/10.1016/j.orgel.2019.105551>

- [23] H. Ullah Khan *et al.*, "Exploring the NH<sub>3</sub> gas sensing efficiency of polyvinylpyrrolidone based tungsten trioxide (PVP/WO<sub>3</sub>) Nanocomposites: A recent progression in the toxic gas sensing materials," *Materials Science and Engineering: B*, vol. 273, pp. 115422, 2021. <https://doi.org/10.1016/j.mseb.2021.115422>.
- [24] I. Tang, R. Sundari, H. Lintang, and L. Yuliati, "Polyvinylpyrrolidone as a New Fluorescence Sensor for Nitrate Ion," *Malaysian Journal of Analytical Sciences*, vol. 20, pp. 288-295, 2016. 10.17576/mjas-2016-2002-09
- [25] K. Mosalagae, D. M. Murape, and L. M. Lepodise, "Effects of growth conditions on properties of CBD synthesized ZnO nanorods grown on ultrasonic spray pyrolysis deposited ZnO seed layers," *Heliyon*, vol. 6, no. 7, pp. e04458, 2020. <https://doi.org/10.1016/j.heliyon.2020.e04458>
- [26] M. Khiari, M. Gilliot, M. Lejeune, F. Lazar, and A. Hadjadj, "Preparation of Very Thin Zinc Oxide Films by Liquid Deposition Process: Review of Key Processing Parameters," *Coatings*, vol. 12, no. 1, pp. 65, 2022.
- [27] S. Paul, J. Sultana, N. R. Saha, G. K. Dalapati, A. Karmakar, and S. Chattopadhyay, "Impact of seed layer annealing on the optoelectronic properties of double-step CBD grown n-ZnO nanowires/p-Si heterojunctions," *Optik*, vol. 228, pp. 166141, 2021. <https://doi.org/10.1016/j.ijleo.2020.166141>
- [28] M. Belhaj, C. Dridi, Y. G. Habba, M. Capo-Chichi, and Y. Leprince-Wang, "Surface morphology evolution with fabrication parameters of ZnO nanowires toward emission properties enhancement," *Physica B: Condensed Matter*, vol. 526, pp. 64-70, 2017. <https://doi.org/10.1016/j.physb.2017.08.034>
- [29] Y. G. Mourzina, Y. E. Ermolenko, T. Yoshinobu, Y. Vlasov, H. Iwasaki, and M. J. Schöning, "Anion-selective light-addressable potentiometric sensors (LAPS) for the determination of nitrate and sulphate ions," *Sensors and Actuators B: Chemical*, vol. 91, no. 1, pp. 32-38, 2003. [https://doi.org/10.1016/S0925-4005\(03\)00063-7](https://doi.org/10.1016/S0925-4005(03)00063-7)
- [30] K. Khun, Z. H. Ibupoto, C. O. Chey, J. Lu, O. Nur, and M. Willander, "Comparative study of ZnO nanorods and thin films for chemical and biosensing applications and the development of ZnO nanorods based potentiometric strontium ion sensor," *Applied Surface Science*, vol. 268, pp. 37-43, 2013. <https://doi.org/10.1016/j.apsusc.2012.11.141>